Activin B Promotes BMSC-Mediated Cutaneous Wound Healing by Regulating Cell Migration Via the JNK–ERK Signaling Pathway

Min Zhang,*[1] Li Sun,*[1] Xueer Wang,* Shixuan Chen,* Yanan Kong,* Nuyun Liu,†
Yinghua Chen,* Qin Jia,* Lu Zhang,†‡ and Lin Zhang*

*Department of Histology and Embryology, School of Basic Medical Sciences, Southern Medical University, Guangzhou, China
†Elderly Health Services Research Center, Southern Medical University, Guangzhou, China
‡Department of Pathophysiology, School of Basic Medical Sciences, Southern Medical University, Guangzhou, China

Bone marrow-derived mesenchymal stem cells (BMSCs) are able to differentiate into various types of skin cells and participate in skin regeneration and repair. Activin signaling can regulate wound healing and reepithelialization. The present study assessed the impact of activin B on BMSC-mediated cutaneous wound healing in rats and explored the possible mechanism involved. We found that CFSE-labeled BMSCs participated in wound healing in vivo, and compared to administration with PBS, activin B, or BMSCs, activin B plus BMSCs significantly promoted wound healing and hair follicle regeneration. Activin B induced actin stress fiber formation and cell migration in BMSCs in vitro. Activation of JNK and ERK, but not p38, was required for activin B-induced actin stress fiber formation and BMSC migration. These results show that activin B may promote BMSC-mediated wound healing by inducing actin stress fiber formation and BMSC migration via the ERK and JNK signal pathways. Combined administration of BMSCs and cytokines may be a promising therapeutic strategy for the management of skin wounds.

Key words: Activin B; Skin; Wound healing; Bone marrow-derived mesenchymal stem cells (BMSCs);
c-JUN NH$_2$-terminal protein kinase (JNK); Extracellular signal regulated kinase (ERK)

INTRODUCTION

Cutaneous wound healing is a complex and coordinated series of events that includes inflammation, new tissue formation, and tissue remodeling (25). Many approaches that accelerate the wound healing process have been developed. However, improving the speed and quality of healing remain a challenging task faced by clinicians. Skin grafting is currently the most effective method for the management of large skin defects. The discovery in recent years that bone marrow-derived mesenchymal stem cells (BMSCs) are able to differentiate into skin cell types and participate in skin regeneration and repair has provided a promising alternative strategy for the treatment of severe skin wounds. Transplantation of BMSCs into full-thickness burn wounds is significantly able to induce epidermal thickening, increase the number of dermal nerve fibers, accelerate wound healing, and greatly improve healing quality (2,10). Moreover, BMSCs participate in wound reepithelialization and the

regeneration of sweat glands and blood vessels (45). Therefore, BMSCs may be considered ideal seeder cells for skin tissue engineering.

A wide variety of growth factors and cytokines are involved in the regulation of all phases of wound healing (44). Activins are members of the transforming growth factor-β (TGF-β) superfamily that exert their biological effects by binding to specific receptors: activin type I receptors (ACVR 1, ACVR 1B, ACVR 1C) and activin type II receptors (ACVR 2A, ACVR 2B) (4,31,32). Three different forms of activin have been identified, including the homodimers activin A (βAβA), activin B (βBβB), and the heterodimer activin AB (βAβB) (43). Three additional activin B subunits (βC, βD, and βE) have been recently identified (30). Strong and persistent induction of activin B has been found in the hyperproliferative epithelia at the wound edge and in the migrating epithelia of the tongue (18). In addition, overexpression of the activin antagonist follistatin or a dominant-negative activin receptor IB

mutant (dnActRIB) delayed wound reepithelialization after skin injury in mice (3,42), implying a critical role of activin B in the regulation of wound healing.

Stem cell-mediated regeneration and repair involve migration of stem cells from the sites where they colonize to wound sites. The process of migration is controlled by chemokines and their receptors (29,37). Many data suggest that the activin/TGF-β pathway might have an important role in the regulation of BMSC functions, and BMSCs and osteoclasts are the main sources of activin (11,14,35,40). Moreover, BMSCs highly express activin receptors on their surfaces (16). However, most of these studies concern the role and signaling mechanisms of activin A and few of activin B. In our previous studies, we found that activin B promoted keratinocyte migration through the c-JUN NH$_2$-terminal protein kinase (JNK)/ mitogen-activated protein kinase (MAPK) pathway and thereby accelerated wound healing (49–51). Furthermore, our recent results indicated that activin B not only promoted epithelial wound closure in vivo through the ras homolog family member A (RhoA)-Rho-associated coiled-coil kinase (ROCK)-c-Jun signaling pathway, but also stimulated the proliferation of hair follicle cells and regeneration of hair follicles at the wound area (19,52). Therefore, we hypothesized that activin B might improve BMSC-mediated wound healing. To test this hypothesis, we assessed the effect of combined administration of BMSCs and activin B on cutaneous wound healing in rats. In addition, we explored the mechanisms underlying the influence of activin B treatment on BMSC-mediated wound healing in vitro. Our study provides a theoretical basis for the development of new strategies for the management of wounds.

MATERIALS AND METHODS

Animals

Twenty-four 8-week-old male and female specific pathogen-free Sprague–Dawley rats (200 ± 20 g) were provided by the Southern Medical University Laboratory Animal Center (Guangzhou, China; SCXK 2006-0015). The Bioethics Committee of Southern Medical University approved all animal procedures, which were in accordance with the National Institutes of Health (NIH) guidelines for the care and use of laboratory animals.

Isolation, Purification, and Labeling of BMSCs

Three 6-week-old male specific pathogen-free Sprague–Dawley rats were killed by cervical dislocation and soaked in 75% ethanol for 5 min (9,24). The femur and tibia were removed under aseptic conditions, washed with sterile phosphate-buffered saline (PBS, Boster, Wuhan, China), and cut at both ends to gain access to the marrow cavity. The bone marrow was flushed out from the marrow cavity by forcing culture medium

[Dulbecco's modified Eagle's medium supplemented with L-tryptophan (L-DMEM) containing 10% fetal bovine serum, both Gibco/Invitrogen, Carlsbad, CA, USA] using a 1-ml syringe (Jiangxihongda, Nanchang, China). Culture medium containing bone marrow cells was centrifuged at $1,500 \times g$ for 5 min, and the supernatants were discarded. Cell pellets were resuspended in L-DMEM containing 10% fetal bovine serum, plated in plastic tissue culture dishes (Corning, Corning, NY, USA), and cultured in a humid atmosphere with 5% CO$_2$ at 37°C. The culture medium was changed 72 h after plating and every 2–3 days thereafter.

For 5-(6)-carboxyfluorescein diacetate succinimidyl ester (CFSE, Invitrogen) labeling, BMSCs at passages 4–5 were cultured in serum-free medium for 12 h. After removing the culture medium, 5 μM CFSE (diluted in 0.1 M PBS) was added and allowed to incubate at 37°C for 15 min. Following CFSE removal, fresh culture medium was added, and the cells were further incubated at 37°C for 30 min.

Immunocytochemistry

BMSCs at passage 3 were seeded in 12-well plates (Corning) at a density of $4–5 \times 10^5$ cells per well. When cells were 90% confluent, the medium was aspirated out, and cells were rinsed with PBS three times. Cells were then fixed in 4% paraformaldehyde (PFA) for 10 min, permeabilized with 0.5% Triton X-100 for 15 min, and blocked with 1% bovine serum albumin (BSA; all Sigma, St. Louis, MO, USA) for 30 min at room temperature. Following incubation with a primary antibody [rabbit anti-rat cluster of differentiation 44 (CD44) polyclonal antibody, 1:10; mouse anti-rat CD90 monoclonal antibody, 1:100; rabbit anti-rat CD29 polyclonal antibody, 1:200; or rabbit anti-rat CD80 polyclonal antibody, 1:100; all from Abcam, Cambridge, UK] at 37°C for 2 h, cells were rinsed with PBS. Incubation with a secondary antibody followed (fluorescently labeled goat anti-rabbit IgG, 1:200; donkey anti-mouse IgG, 1:200; goat anti-rabbit IgG, 1:200; or goat anti-mouse IgG, 1:200; all from Invitrogen) at room temperature for 1 h. After washing with PBS, cells were counterstained with Hoechst 33258 (1:500; Sigma) for 10 min, washed again with PBS, mounted, and examined via fluorescence microscopy.

Wound Healing Model

Rats were anesthetized by an intraperitoneal injection of 10% chloral hydrate (w/v; 0.003 ml/g body weight; Sigma). After the dorsal hair was depilated using a honey and wax mixture (Mayllice; CP-WAX Srl, Piacenza, Italy), a 1×1-cm square was delineated on the skin with Skin Marker (SM10; Kearing, Shanghai, China); then full-thickness skin wounds 1 cm^2 in area were created on the dorsal right and left shaved skin with sterile scissors along

the square after povidone–iodine disinfection (Hengjian, Guangzhou, China). After wound creation and recovery, the rats were given free access to food and water.

Rats were randomly divided into four treatment groups and 0.4 ml PBS (vehicle control), 10 ng/ml activin B (R&D Systems, Minneapolis, MN USA), $6–8 \times 10^6$/ml BMSCs, or 10 ng/ml activin B + $6–8 \times 10^6$/ml BMSCs was applied to the site surrounding the wound once daily on days 1–3 after wounding. Wound areas were measured photographically every day after wounding, and the rate of wound closure was calculated as wound closure rate (%) = [(original wound area − open area on final day)/ original wound area] × 100% (52).

Hematoxylin and Eosin (H&E) Staining and Histological Evaluation

On postoperative days 3, 7, and 14, the complete wound with a 0.5-cm margin was carefully removed, rinsed in PBS, fixed in 4% PFA, rinsed again in PBS, dehydrated in a graded ethanol series, cleared in dimethylbenzene (Boster), and embedded in paraffin. Five-micrometer sections were prepared, deparaffinized in dimethylbenzene, and rehydrated. The samples were divided in half between the longest and the shortest diameters of the wound, and the wound section parallels the anterior–posterior axis of the mouse. For histological assessment, we cut serial sections (0.5 μm), and for each adjacent pair, taken from the wound center or margin, one section was stained with hematoxylin and eosin (H&E; MaiXin-Bio, Fuzhou, China) in accordance

with standard procedures and the other with Masson's trichrome staining (MaiXin-Bio, Fuzhou, China) (12) and fibroblast-specific protein (FSP-1) (Millipore, Billerica, MA, USA) and CD31 (R&D Systems). Histological evaluation of wound healing was made in accordance with the criteria listed in Table 1. From each group at different time points were selected five samples for epidermal layer and basal cell layer evaluation or high-power field (20× for capillary; 40× for fibroblast vessels). The immunohistochemistry-positive cells/area, mm² = positive cell number/high-power field area.

Phallotoxin Staining

BMSCs at passage 4 were seeded in 24-well plates (Corning) with one coverslip (Fisher Scientific, Shanghai, China) in each well at a density of 4×10^5 cells/well. Cells were serum starved for 12 h and divided into eight treatment groups. The negative and positive control treatments consisted of incubation in DMEM containing PBS, and 10 ng/ml activin B, respectively. The six experimental treatments consisted of 30-min incubations in one of three inhibitors (each at 5 μM), followed by incubation in either DMEM or 10 ng/ml activin B in DMEM. The three inhibitors were the JNK-specific inhibitor SP600125 (Santa Cruz, Dallas, TX, USA), the p38-specific inhibitor SB202190 (Santa Cruz), and the extracellular signal-regulated kinase (ERK)-specific inhibitor SL327 (Santa Cruz).

At 30, 120, 240, or 360 min after treatment, coverslips were removed, and cells were fixed in 4% PFA, permeabilized with 0.1% Triton X-100 for 5 min, blocked with

Table 1. Criteria for Histological Evaluation of Cutaneous Wound Healing (1,7,8)

Project	Scores	Evaluation
Epidermal layer	1±	Thin, a small part of wound repaired
	2±	Thick, wound partially repaired
	3±	Epidermal keratinization, epidermal layer repaired
Basal cell layer	1±	Basal cells are not obvious and are disorderly
	2±	Basal cells tend to be columnar and close together
	3±	Basal cells are columnar and are closely arranged in a single layer
Granulation tissue thickness	1±	Thin granular layer: 0–30/Hp* of fibroblasts, collagen fibers without direction
	2±	Moderate granulation layer: 30–50/Hp of fibroblasts, collagen fibers arranged orderly
	3±	Thick granulation layer: 50–80/Hp of fibroblasts, a large amount of collagen fibers arranged orderly
	4±	Very thick granulation layer: more than 80 Hp of fibroblasts, excessive collagen fibers
Angiogenesis	1±	Altered angiogenesis (0–2 vessels per site)
	2±	Few newly formed capillary vessels (3–6 per site)
	3±	Newly formed capillary vessels (7–10 per site)
	4±	Newly formed and well-structured capillary vessels (10 per site) vertically disposed toward the epithelium and at the wound margins

*Note: Hp: 40×; 1±, 2±, 3±, and 4± means 0.5 to 1.5, 1.5 to 2.5, 2.5 to 3.5, and 3.5 to 4.5.

1% BSA for 20 min at room temperature, and stained with phallotoxins (phalloidin; Invitrogen). After washing with PBS, cells were counterstained with Hoechst 33258 (dilution 1:500) for 10 min, washed again with PBS, mounted, and examined by fluorescence microscopy.

Scratch Wound Healing Assay

BMSCs at passage 4 were seeded in 12-well plates at a density of $4–5 \times 10^5$ cells per well. When cells grew to 90% confluence, the medium was aspirated away, and cells were serum starved for 12 h. Cells were divided into eight groups and treated as described above. A scratch wound was created with a micropipette tip. The wounds were photographed at 0, 12, 24, 36, 48, 60, and 72 h after wounding. Assays were performed in quadruplicate.

Transwell Migration Assay

BMSCs at passage 4 were serum starved for 12 h, resuspended in serum-free medium, and adjusted to a density of 1×10^6 cells/ml. One hundred microliters of BMSCs was placed in the upper chamber of Transwell plates (Corning, Corning, NY, USA). Serum-free L-DMEM, with or without activin B, was added to the lower chamber. Prior to the addition of BMSCs, preheated serum-free L-DMEM (300 μl) was added to the upper chamber and allowed to incubate for 1 h at 37°C. After BMSCs were incubated for 24 h at 37°C, migrated cells were collected from the lower chambers, stained with crystal violet (Beyotime, Haimen, China), photographed (20×), and from each group was selected five samples for counting.

Western Blot

BMSCs at passage 4 were serum starved for 12 h, washed twice with Hank's solution (Beyotime) at 37°C, and cultured in DMEM containing either PBS or 10 ng/ml activin B. At 10, 30, or 120 min after treatment, cells were harvested and used to prepare total protein lysates. Total protein contents were determined with the bicinchoninic acid assay (Beyotime).

Twenty-five micrograms of protein from each sample was resolved via 5% sodium dodecyl sulfate-polyacrylamide gel electrophoresis (SDS-PAGE; Fdbio Science, Hangzhou China) and transferred to poly-vinylidene fluoride membranes (Millipore). The blots were blocked with 5% skim milk (Genebase, Guangzhou, China) and incubated with a primary antibody: p-JNK (1:5,000; Promega, Madison, WI, USA) p-ERK or p-p38 (1:1,000; Cell Signaling Technologies, Danvers, MA, USA) at 4°C overnight, followed by incubation with a secondary antibody (Cell Signaling Technologies) for 1 h at room temperature. Antibody binding was detected using an enhanced chemiluminescence kit (Millipore). The blots were then incubated in a commercial stripping solution (Pierce protein; Thermo, Rockford, IL, USA) for

10 min and reprobed with antibodies against JNK, ERK, and p38 (1:1,000; Cell Signaling Technologies).

The bands were quantified using Quantity One software (Bio-Rad, Hercules, CA, USA) by measuring the band intensity.

Statistical Analyses

Statistical analyses were performed using SPSS13.0 software (IBM, Armonk, NY, USA). Data were expressed as mean ± standard deviation. Wound closure rate was evaluated by single factor repeated measurement. If there was an interaction effect between time and group, the data would be evaluated by separate effects analysis, and if there was no interaction effect between time and group, they would be evaluated by repeated measures analysis in the group and by one-way ANOVA among the groups as well, and then the post hoc tests after ANOVA were least-significant difference (equal variances assumed) and Dunnett's T3 (equal variances not assumed). The histological evaluation of cutaneous wound healing and the band relative intensity were compared using factorial analysis. As mentioned above, if there was an interaction effect between time and group, they would be evaluated by separate effects analysis, and if there was no interaction effect between time and group, they would be evaluated by independent-samples t test or one-way ANOVA, and then the post hoc tests after ANOVA were least-significant difference (equal variances assumed) and Dunnett's T3 (equal variances not assumed). The number of BMSCs/ mm^2 (SE) was evaluated by independent samples t test. Differences were significant with $p < 0.05$.

RESULTS

Activin B Promotes BMSC-Mediated Wound Healing

To test our hypothesis that activin B can improve BMSC-mediated wound healing, we first created a full-thickness wound healing model in rats. BMSCs were identified based on reported criteria such as the presence of CD90^{+}, CD44^{+}, CD29^{+}, and CD80^{−} (6,33,39,47). We then evaluated whether activin B promotes BMSC-mediated wound healing by applying PBS, activin B, BMSCs, or activin B plus BMSCs to wound sites and monitoring wound closure. Compared with PBS, activin B, or BMSCs, activin B plus BMSCs significantly promoted wound healing (Fig. 1A). On days 7 and 14 after treatment, the rates of wound closure were significantly higher in the activin B plus BMSC group than in the PBS, BMSC, and activin B groups (Fig. 1B).

Qualitative data regarding histological evaluation according to the criteria in Table 1 (1,7,8) at day 14 are shown in Figure 2. Compared with other groups, in the BMSC plus activin B group on day 7, the epidermal layers were thicker, and most of the basal cells tended to be columnar and close together. Also, newly formed
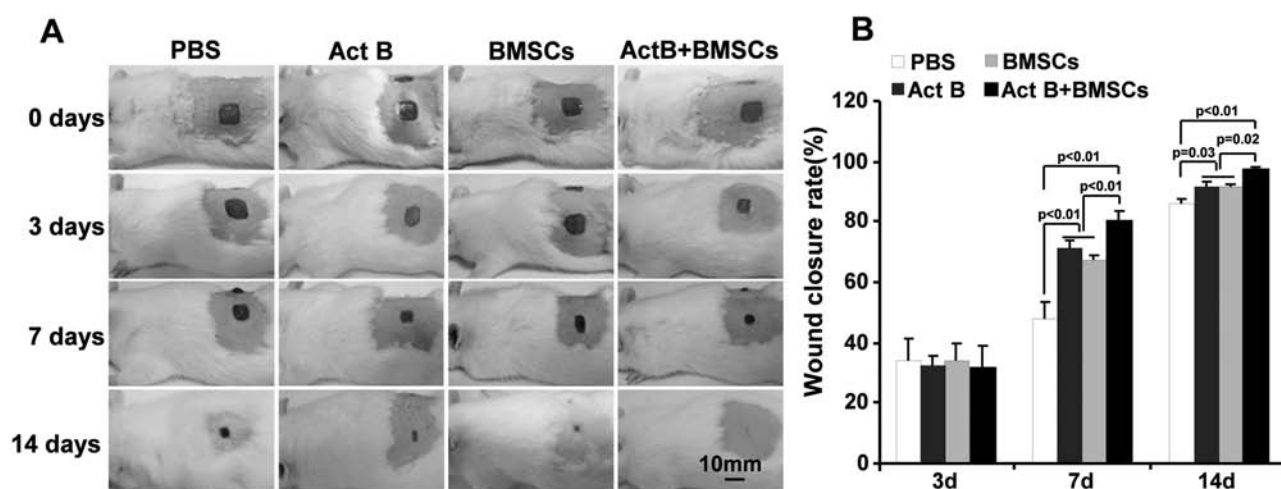
Figure 1. Activin B promotes BMSC-mediated wound healing. After wounding, four groups of rats were administered phosphate-buffered saline (PBS), activin B (Act B), bone marrow-derived mesenchymal stem cells (BMSCs), and Act B+BMSCs, respectively. The wound healing status was monitored every day, and wound closure rate was calculated. (A) Representative images taken at the indicated time points after wounding. (B) Comparison of the rate of wound closure among the four groups ($n=6$).
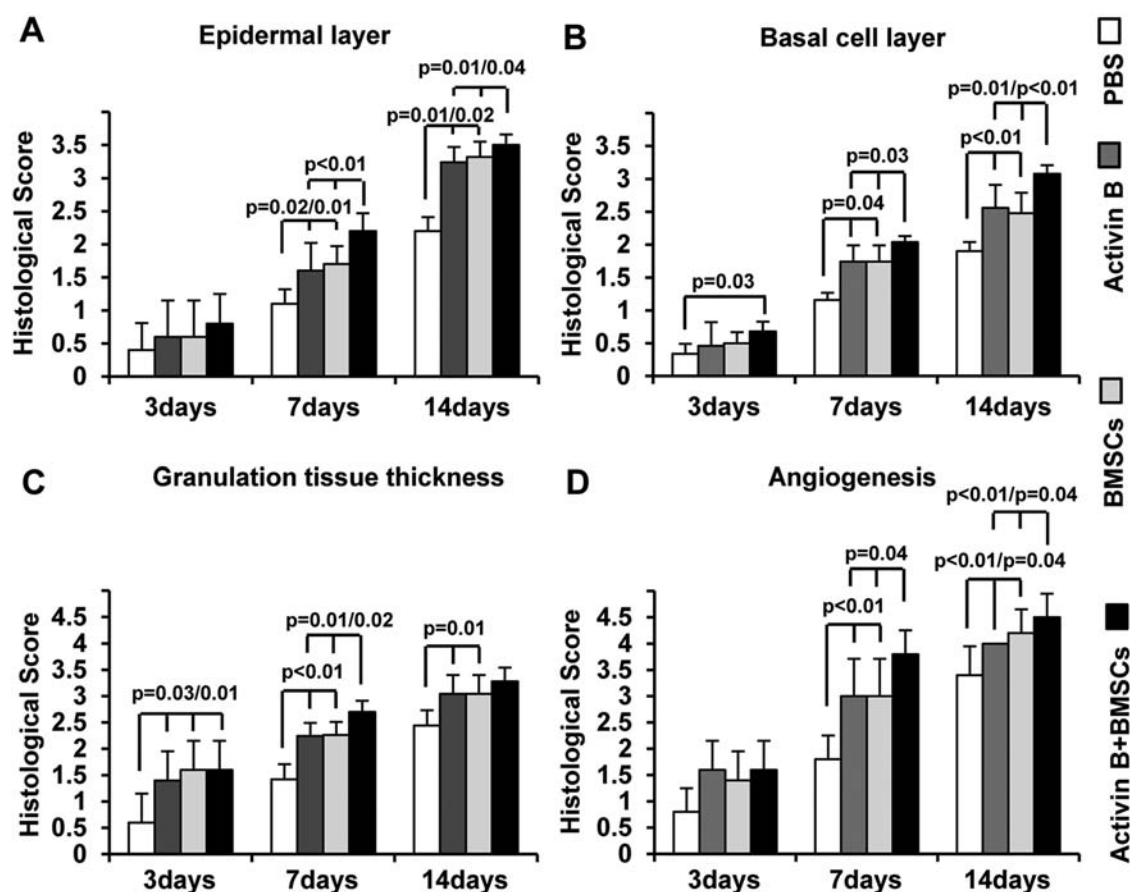

Figure 2. Time course of histological scores in treatment groups. Each point represents the mean±SD histological score of five experiments. On days 3, 7, and 14, sections 5 μm thick of paraffin-embedded tissues were mounted on glass slides and stained with hematoxylin and eosin (H&E) and fibroblast-specific protein 1 (FSP-1) and/or cluster of differentiation 31 (CD31) by immunohistochemistry to identify fibroblasts and angiogenesis for the histological evaluation of granulation tissue thickness and angiogenesis (data not shown). The parameters measured were epidermal layer (A) and basal cell layer (B), granulation tissue thickness (C), and angiogenesis (D). The margins of the wound in each of the sections, as well as normal control wounds, were used as comparisons for scoring (Table 1).

capillary vessels were observed in greater numbers compared with other groups in the dermis of the entire wound area on day 7. On day 12, the wound reepithelialization was completed in the BMSC plus activin B group. On day 14, in the BMSC plus activin B group, the epidermal layers showed keratinization; most basal cells were columnar in a single and closely arranged layer. Dermal regeneration was characterized by thick granulation tissue rich in more than 50/Hp of fibroblasts and a large number of collagen fibers arranged in order. However, there was no significant difference in the number of newly formed capillary vessels among the four groups (Fig. 3A2–D2). In the activin B and BMSC groups on day 14, the wound

reepithelialization was completed, but in the PBS group, epidermal elongation only speeded over $83 \pm 3\%$ of the wound surface (Fig. 3A–C). Unlike the PBS and BMSC groups, regeneration of hair follicles was observed in the activin B and combination groups (Fig. 3A1–D1).

We next examined wound healing in rats transplanted with CFSE-labeled BMSCs using an in vivo imager. On days 3 and 7 after cell transplantation, CFSE green fluorescence was detected (CFSE+) in rats administered with BMSCs alone or in combination with activin B, but not in those administered with activin B or PBS. In frozen sections, CFSE+ BMSCs had been incorporated into wound sites on day 3 (Fig. 4). On day 7, CFSE+ BMSCs
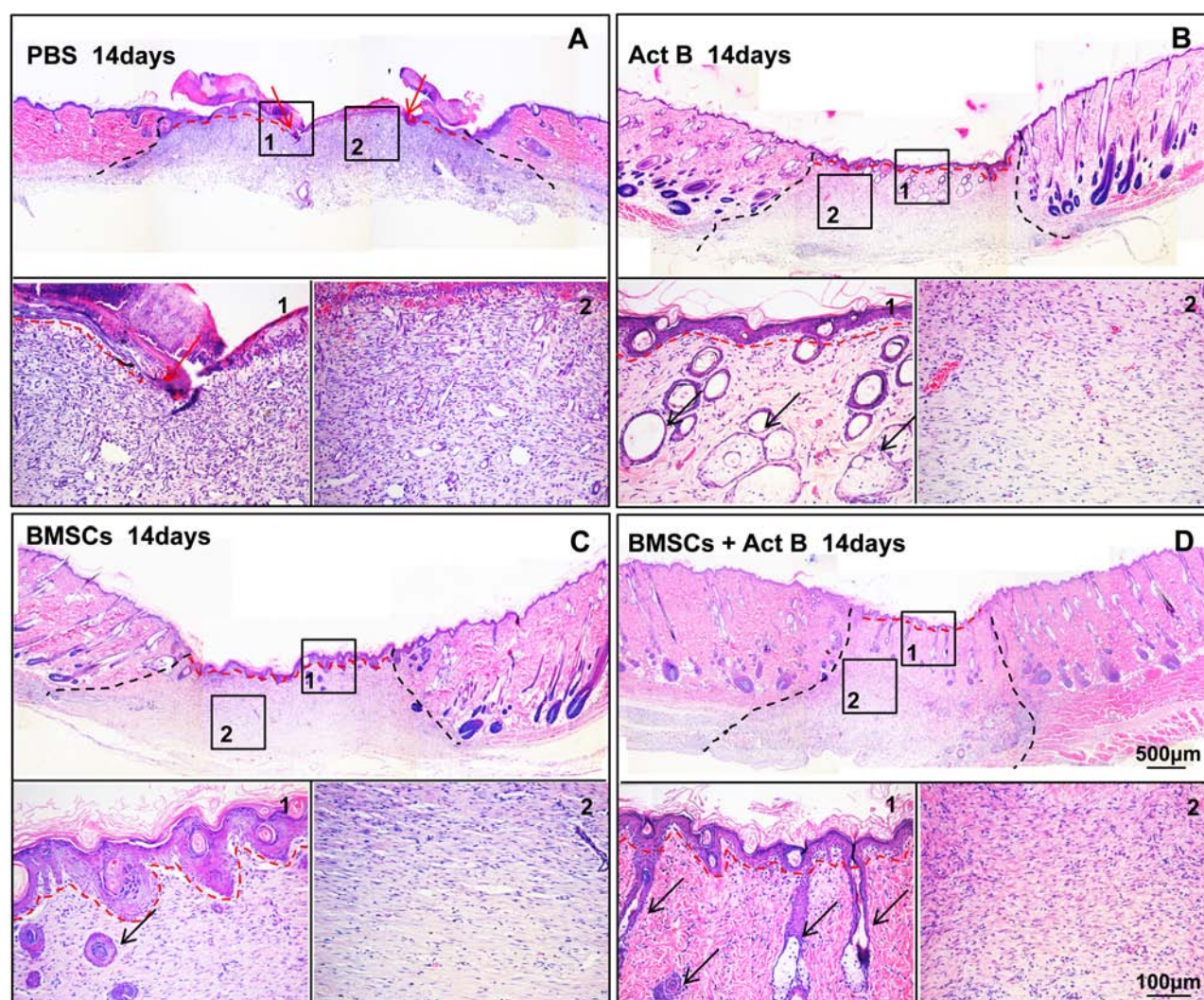

Figure 3. H&E staining of the skin tissues surrounding wound sites showed wound reepithelialization and hair follicle regeneration on day 14 postwounding. (A) Red arrows indicate the position in the epithelial edge (A1). Representative images for the different treatment groups: (A) PBS, (B) Act B, (C) BMSCs, and (D) BMSCs+Act B. The black dotted line shows the edge of granulation tissue, red dotted line shows the reepithelialization of epithelial, and black arrows indicate the hair follicle and glands in the wound site. Insets of main figures represent (1) wound reepithelialization and (2) granulation tissue.
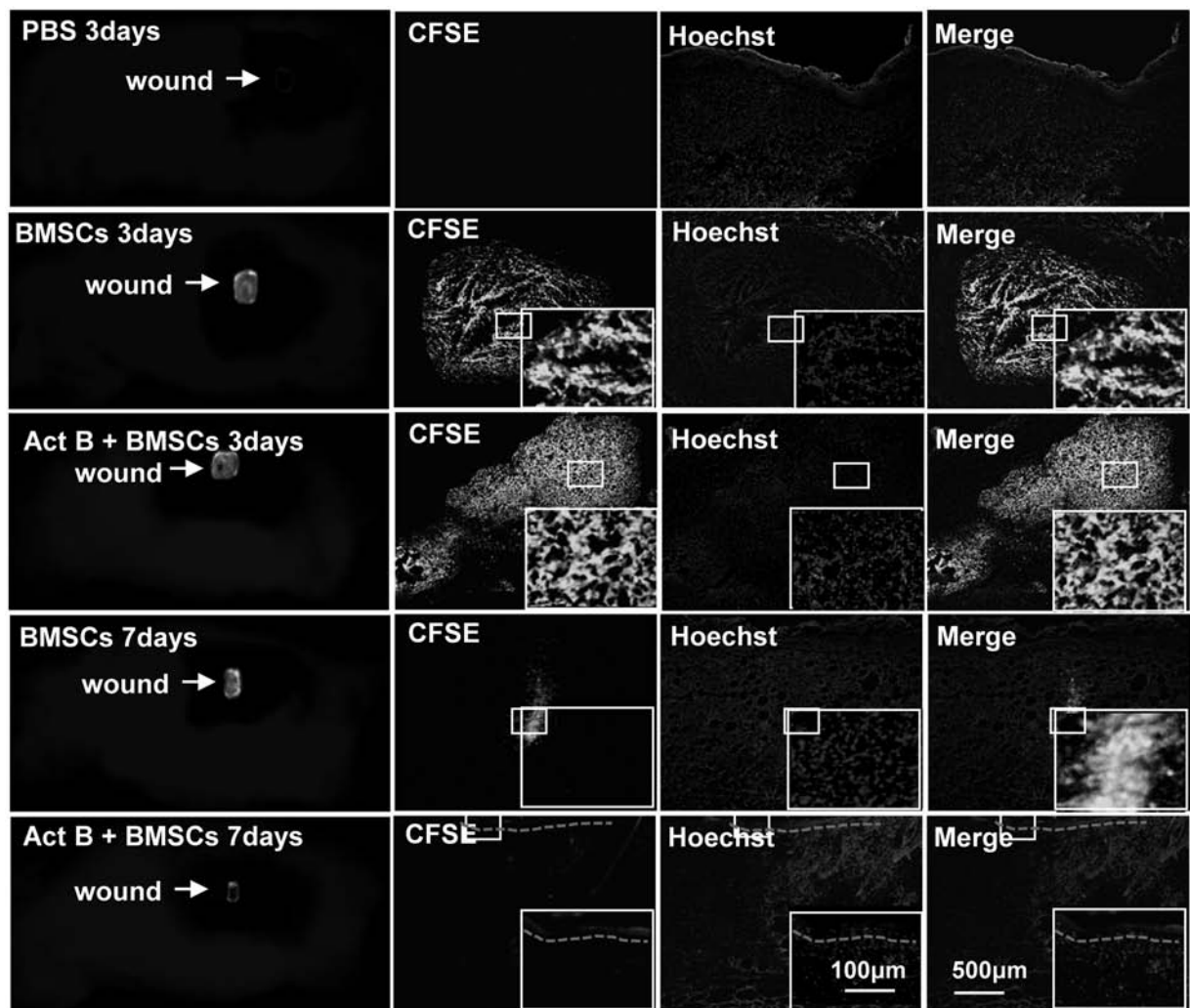
Figure 4. BMSCs participate in cutaneous wound healing. CFSE [5-(6)-carboxyfluorescein diacetate succinimidyl ester]-labeled BMSCs were administered to the wound sites in rats of different treatment groups for 3 consecutive days. On days 3 and 7 after administration, CFSE-labeled BMSCs (arrow) were observed with an in vivo imager or examined by fluorescence microscopy of frozen sections, gray dotted line show the reepithelialization of the epithelium.

had disappeared from the wound sites and migrated to the wound margin in rats administered with BMSCs plus activin B. In contrast, some CFSE⁺ BMSCs were still observed at wound sites in rats administered with BMSCs without activin B. Taken together, these data suggest that combined activin B and BMSCs could not only promote wound reepithelialization and healing but also stimulate the regeneration of hair follicles.

Activin B Promotes BMSC Migration Possibly by Inducing Actin Stress Fiber Formation

The cytoskeleton comprises three principal polymer systems: microtubules, microfilaments, and intermediate filaments. Microfilaments are composed of actin protein and have a crucial role in cell migration and contraction (21). To investigate whether activin B regulates actin

stress fiber formation in BMSCs, we examined the distribution and formation of actin stress fibers in BMSCs treated with activin B by phallotoxin (phalloidin) staining. Actin stress fibers were mainly distributed along the membrane, 30 min after treatment (Fig. 5A). At 2 and 4 h, numerous actin stress fibers were arranged across the cell bodies. At 6 h, only a few actin stress fibers were seen at the periphery of cells. In contrast, the distribution and number of actin stress fibers showed no significant changes throughout the process in PBS-treated cells. Apparently, activin B induced actin stress fiber formation in BMSCs.

Since actin polymerization is very important in cell migration (21), we next examined the impact of activin B on the migration of BMSCs with the scratch wound healing and Transwell migration assays. Many BMSCs
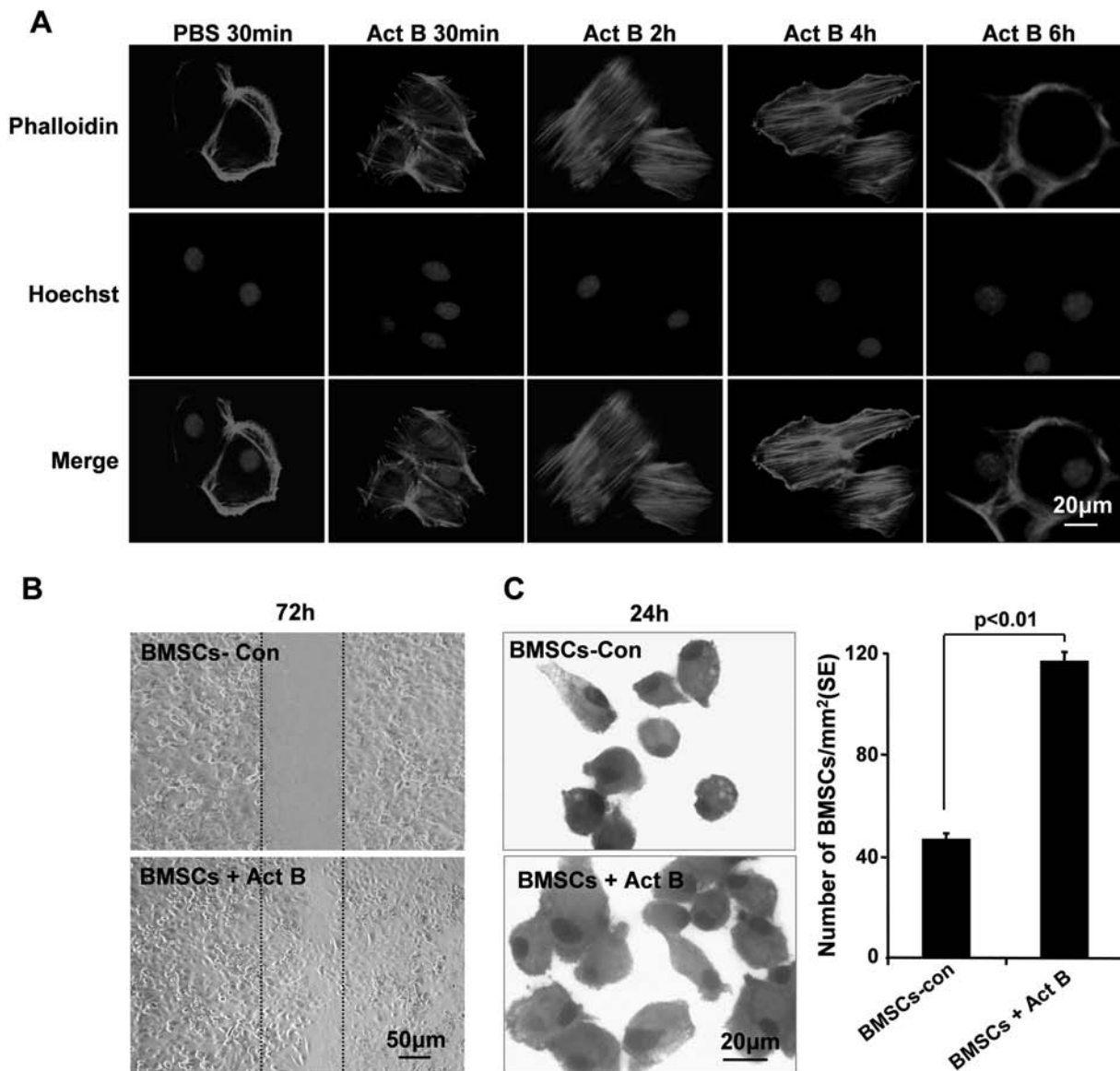
Figure 5. Activin B induces actin stress fiber formation and BMSC migration. (A) Activin B induces actin stress fiber formation in BMSCs. BMSCs were serum starved for 12 h and treated with10 ng/ml activin B for 0.5, 2, 4, or 6 h. After treatment, phallotoxin staining (phalloidin) was performed to stain actin. Nuclei were counterstained with Hoechst 33258. (B) Activin B promoted the migration of BMSCs to the scratch wound. BMSCs were serum starved for 12 h and treated with 10 ng/ml activin B or PBS. A scratch wound was then created. At 72 h after wounding, the wounds were photographed. (C) Analysis of activin B treatment on BMSC migration by Transwell migration assay. BMSCs treated with activin B or PBS were subjected to Transwell migration assays. Six visual fields (40×) were randomly chosen from each group to compare the number of cells that migrated into the lower chamber.

treated with 10 ng/ml activin B migrated to the scratch wound 72 h after the scratch, while few PBS-treated BMSCs were found in the scratch wound (Fig. 5B). In the Transwell migration assay, the number of cells that migrated to the lower chamber was significantly higher in BMSCs treated with 10 ng/ml activin B than in PBS-treated BMSCs (Fig. 5C). Taken together, these data suggest that activin B induces actin stress fiber formation and BMSC migration.

Activation of JNK and ERK, But Not p38, Was Required for Activin B-Induced Actin Stress Fiber Formation and BMSC Migration

The MAPK signaling pathway plays a key role in the regulation of cell migration and wound healing (17,20,41,46). To examine whether the MAPK signaling pathway is involved in activin B-induced BMSC migration, we determined the phosphorylation status of JNK, ERK, and p38 in BMSCs treated with 10 ng/ml

activin B or PBS. The levels of JNK and ERK phosphorylation were significantly increased 10 min after activin B treatment and reached maximum at 30 min (Fig. 6A, B). Two hours later, JNK phosphorylation returned to baseline, and ERK phosphorylation slightly decreased from the peak. In contrast, p38 phosphorylation showed no significant changes after activin B treatment (data not shown).

To further determine whether JNK and ERK signaling mediates activin B-induced actin stress fiber formation and BMSC migration, specific inhibitors were used to treat BMSCs, 2 h after activin B treatment. Both SP600125, a specific inhibitor of JNK, and SL327, a specific inhibitor of ERK, significantly inhibited activin B-induced actin stress fiber formation (Fig. 7A). In contrast, the p38-specific inhibitor SB202190 showed no
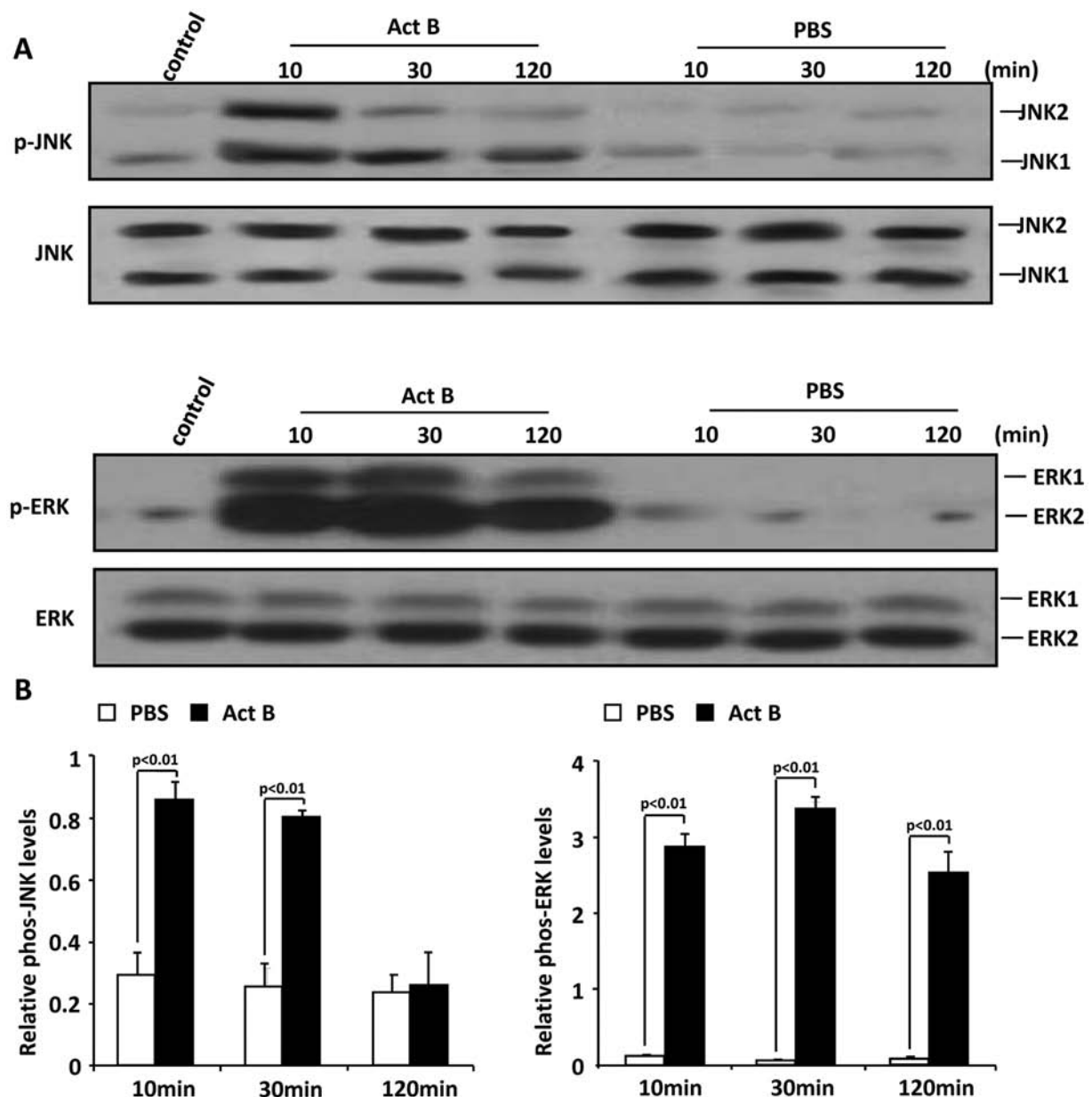

Figure 6. Activin B stimulates JNK and ERK phosphorylation in BMSCs. BMSCs were serum starved for 12 h and treated with 10 ng/ml activin B for 10, 30, or 120 min. Total protein extracts were prepared and analyzed by sodium dodecyl sulfate-polyacrylamide gel electrophoresis (SDS-PAGE) and Western blot to detect the phosphorylation levels of c-JUN NH2-terminal protein kinase (JNK) and extracellular signal regulated kinase (ERK). (A) Representative Western blot images for JNK and ERK. (B) Densitometric analysis of Western blots compared by t test.
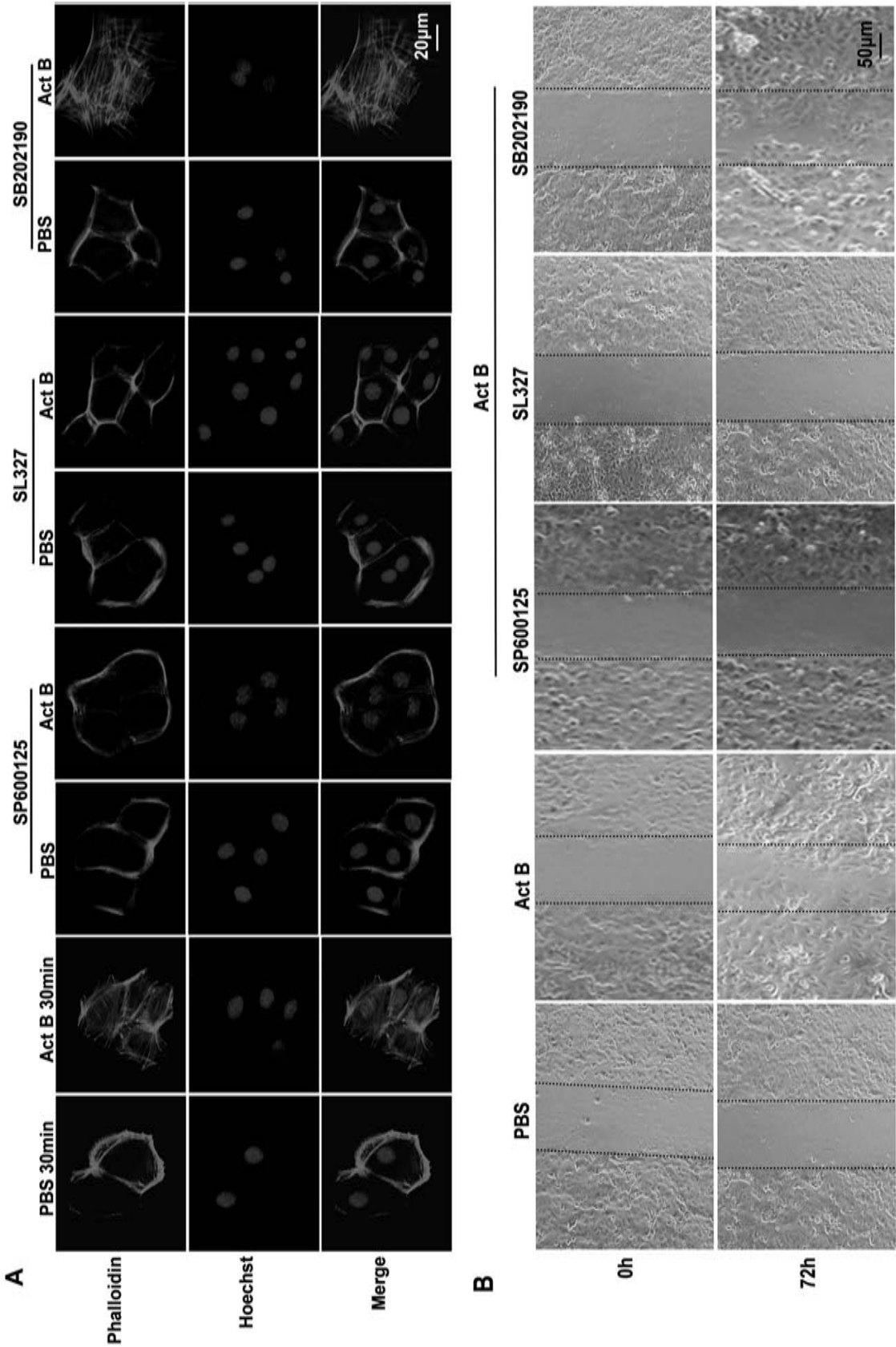
Figure 7. Activin B induces actin stress fiber formation and BMSC migration by activating JNK and ERK. (A) Activation of JNK and ERK, but not p38, is required for activin B-induced actin stress fiber formation. BMSCs were serum starved for 12 h, pretreated with JNK inhibitor SP600125, ERK inhibitor SL327, or p38 mitogen-activated protein kinase (p38 MAPK) inhibitor SB202190 for 30 min, and then treated with 10 ng/ml or PBS. Two hours later, phallotoxin staining was performed. (B) Activation of JNK and ERK, but not p38, is required for activin B-mediated BMSC migration to the scratch wound. After BMSCs were treated with each inhibitor and treated with 10 ng/ml activin B or PBS, a scratch wound was created. At 72 h after wounding, the wounds were photographed.

significant impact. Similar results were also obtained in the scratch wound healing assays. Many BMSCs treated with combined activin B and SB202190 had migrated to the scratch wound 72 h after the scratch, but there were very few PBS-treated BMSCs, BMSCs treated with combined activin B and SP600125, or those treated with combined activin B and SL327 in the scratch wound (Fig. 7B). Collectively, these data suggest that activation of JNK and ERK, but not p38, is required for activin B-induced actin stress fiber formation and BMSC migration.

DISCUSSION

Faster healing and better healing quality are two challenging issues for researchers in the fields of wound healing and tissue regeneration. Fast wound healing reduces the incidence of many wound complications, while good healing quality ensures the restoration of anatomical continuity and functional integrity of the wounded tissue. Thus, the development of better strategies for promoting wound healing is of great clinical importance.

BMSCs can not only be transplanted and have low immunogenicity, but they also possess immunomodulatory properties (22,23,28,38). As seeder cells, BMSCs can differentiate into multiple cell and tissue types and participate in cutaneous wound healing (36). In addition, they secrete biologically active substances like cytokines, which can improve the wound microenvironment and promote wound healing (5,27,34). However, BMSCs must migrate to wound sites before they can be involved in the repair process, and the ability of BMSCs to migrate to injured tissues has been demonstrated in many previous studies (2,10,45). We examined the impact of combined administration of BMSCs and activin B on wound healing in a rat model in the present study. We found that activin B did indeed promote BMSC-mediated wound healing in vivo. In addition, our in vitro results indicated that activin B induced actin stress fiber formation and cell migration in BMSCs. Activation of JNK and ERK, but not p38, was required for activin B-induced actin stress fiber formation and BMSC migration. Taken together, these findings suggest that activin B regulates BMSC-induced cell migration in wound healing through the JNK-ERK signaling pathway.

As BMSCs highly express activin receptors on their surface, and activin B can promote wound healing, reduce the formation of hypertrophic scars, and improve healing quality (15), we hypothesized that activin B could promote BMSC-mediated wound healing. In this study, we found that combined administration of BMSCs and activin B significantly accelerated wound healing and promoted hair follicle regeneration. Moreover, we found that activin B promoted BMSC migration, possibly by inducing actin stress fiber formation. Consistent with our results, a previous study showed that TGF-β could promote migration of BMSCs into vascular smooth muscle

cells in a rat carotid injury model (48). Taken together, these findings suggest that combined administration of seeder cells and cytokines represent a feasible strategy for improving healing velocity and quality.

Currently, multiple cell signaling pathways have been implicated in the regulation of BMSC migration. The migration of MSCs in response to a tumor cell-conditioned medium requires stromal cell-derived factor 1 (SDF1)-mediated activation of signal transducers and activators of transcription 3 (STAT3) and focal adhesion kinase (FAK) (13). Sphingosine-1-phosphate (S1P)-induced mobilization of BMSCs needs the cooperation of matrix metalloproteinases with the RhoA/Rho-kinase and mitogen-activated protein kinase kinase-1 (MAPKK1)/ERK signaling pathways (26). In addition, in our previous studies, we demonstrated that activin/TGF-β controls actin cytoskeleton reorganization and epithelial cell migration in vitro through the MAPK pathway, and activin B regulates wound healing in vivo through the RhoA–JNK pathway (50). In this study, we found that activation of JNK and ERK, but not p38, is required for activin B-induced actin stress fiber formation and BMSC migration. These data highlight the complex pleiotropic mechanisms by which BMSC migration is regulated.

In conclusion, the present study showed the beneficial effect of activin B in BMSC-mediated wound healing. In addition, we found that activin B promoted BMSC migration, possibly by inducing actin stress fiber formation via the ERK and JNK signal pathways. Combined administration of BMSCs and cytokines may be a promising therapeutic strategy for the management of wounds.

REFERENCES

1. Altavilla, D.; Saitta, A.; Cucinotta, D.; Galeano, M.; Deodato, B.; Colonna, M.; Torre, V.; Russo, G.; Sardella, A.; Urna, G.; Campo, G. M.; Cavallari, V.; Squadrito, G.; Squadrito, F. Inhibition of lipid peroxidation restores impaired vascular endothelial growth factor expression and stimulates wound healing and angiogenesis in the genetically diabetic mouse. Diabetes 50:667–674; 2001.

2. Badiavas, E. V.; Abedi, M.; Butmarc, J.; Falanga, V.; Quesenberry, P. Participation of bone marrow derived cells in cutaneous wound healing. J. Cell. Physiol. 196:245–250; 2003.

3. Bamberger, C.; Scharer, A.; Antsiferova, M.; Tychsen, B.; Pankow, S.; Müller, M.; Rülicke, T.; Paus, R.; Werner, S. Activin controls skin morphogenesis and wound repair predominantly via stromal cells and in a concentration-dependent manner via keratinocytes. Am. J. Pathol. 167: 733–747; 2005.

4. Chang, H.; Brown, C. W.; Matzuk, M. M. Genetic analysis of the mammalian transforming growth factor-beta super-family. Endocr. Rev. 23:787–823; 2002.

5. Cheng, G.; Youssef, B. B.; Markenscoff, P.; Zygourakis, K. Cell population dynamics modulate the rates of tissue growth processes. Biophys. J. 90:713–724; 2006.

6. Dominici, M.; Le Blanc, K.; Mueller, I.; Slaper-Cortenbach, I.; Marini, F.; Krause, D.; Deans, R.; Keating, A.; Prockop, D. J.; Horwitz, E. Minimal criteria for defining multipotent mesenchymal stromal cells. The International Society for Cellular Therapy position statement. Cytotherapy 8:315–317; 2006.

7. Du, Y. R.; Fu, X. B.; Li, C. B.; Sun, T. F.; Fang, L. J.; Chen, W. Role of basic fibroblast growth factor combined with mesenchymal stem cells in promoting wound healing. Chin. J. Trauma 21:290–294; 2005.

8. Eldad, A.; Weinberg, A.; Breiterman, S.; Chaouat, M.; Palanker, D.; Ben-Bassat, H. Early nonsurgical removal of chemically injured tissue enhances wound healing in par-tial thickness burns. Burns 24:166–172; 1998.

9. Friedenstein, A. J.; Piatetzky-Shapiro, I. I.; Petrakova, K. V. Osteogenesis in transplants of bone marrow cells. J. Embryol. Exp. Morphol. 16:381–390; 1966.

10. Fu, X. B.; Qu, Z. L.; Sheng, Z. Y. Potentiality of mesenchy-mal stem cells in regeneration of sweat glands. J. Surg. Res. 136:204–208; 2006.

11. Fujita, T.; Epperly, M. W.; Zou, H.; Greenberger, J. S.; Wan, Y. Regulation of the anaphase-promoting complex-separase cascade by transforming growth factor-beta mod-ulates mitotic progression in bone marrow stromal cells. Mol. Biol. Cell 19:5446–5455; 2008.

12. Gamble, M. The hematoxylins and eosin. In: Bancroft, J. D.; Gamble, M., eds. Theory and Practice of Histological Techniques 6th edition. Beijing, China: Peking University Medical Press Publisher. 2008:121–134.

13. Gao, H.; Priebe, W.; Glod, J.; Banerjee, D. Activation of signal transducers and activators of transcription 3 and focal adhesion kinase by stromal cell-derived factor 1 is required for migration of human mesenchymal stem cells in response to tumor cell-conditioned medium. Stem Cells 27:857–865; 2009.

14. Gruber, R.; Mayer, C.; Schulz, W.; Graninger, W.; Peterlik, M.; Watzekm, G.; Luyten, F. P.; Erlacher, L. Stimulatory effects of cartilage-derived morphogenetic proteins 1 and 2 on osteogenic differentiation of bone marrow stromal cell. Cytokine 12:1630–1638; 2000.

15. Gurtner, G. C.; Werner, S.; Barrandon, Y.; Longaker, M. T. Wound repair and regeneration. Nature 453:314–321; 2008.

16. Hennig, T.; Lorenz, H.; Thiel, A.; Goetzke, K.; Dickhut, A.; Geiger, F.; Richter, W. Reduced chondrogenic potential of adipose tissue derived stromal cells correlates with an altered TGFbeta receptor and BMP profile and is overcome by BMP-6. J. Cell. Physiol. 211:682–691; 2007.

17. Huang, C.; Rajfur, Z.; Borchers, C.; Schaller, M. D.; Jacobson, K. JNK phosphorylates paxillin and regulates cell migration. Nature 424:219–223; 2003.

18. Hubner, G.; Hu, Q.; Smola, H.; Werner, S. Strong induction of activin expression after injury suggests an important role of activin in wound repair. Dev. Biol. 173:490–498; 1996.

19. Jia, Q.; Zhang, M.; Kong, Y. N.; Chen, S. X.; Chen, Y. H.; Wang, X. E.; Zhang, L.; Lang, W. Y.; Zhang, L.; Zhang, L. Activin B promotes the initiation and development of hair follicles in mice. Cells Tissues Organs 198:318–326; 2013.

20. Kavurma, M. M.; Khachigian, L. M. ERK, JNK, and p38 MAP kinases differentially regulate proliferation and migration of phenotypically distinct smooth muscle cell subtypes. J. Cell. Biochem. 89:289–300; 2003.

21. Lauffenburger, D. A.; Horwitz, A. F. Cell migration: A physically integrated molecular process. Cell 84:359–369; 1996.

22. Le Blanc, K. Mesenchymal stromal cells: Tissue repair and immune modulation. Cytotherapy 8:559–561; 2006.

23. Le Blanc, K.; Ringden, O. Immunomodulation by mesen-chymal stem cells and clinical experience. J. Intern. Med. 262:509–525; 2007.

24. Li, X. F.; Zhao, J. M.; Su, W.; Cui, X. R.; Luo, S. X.; Ma, A. G. Culture and identification of rat bone marrow mes-enchymal stem cells. J. Clin. Rehabil. Tissue Eng. Res. 15:1721–1725; 2011.

25. Martin, P. Wound healing–Aiming for perfect skin regen-eration. Science 276:75–81; 1997.

26. Meriane, M.; Duhamel, S.; Lejeune, L.; Galipeau, J.; Annabi, B. Cooperation of matrix metalloproteinases with the PhoA/Rho kinase and mitogen-activated protein kinase kinase-1/extracellular signal-regulated kinase signaling pathways is required for the sphingosine-1-phosphate-induced mobilization of marrow-derived stromal cells. Stem Cells 24:2557–2565; 2006.

27. Nakagawa, H.; Akita, S.; Fukui, M.; Fujii, T.; Akino, K. Human mesenchymal stem cells successfully improve skin-substitute wound healing. Br. J. Dermatol. 153:29–36; 2005.

28. Nasef, A.; Ashammakhi, N.; Fouillard, L. Immunomodulatory effect of mesenchymal stromal cells: Possible mechanisms. Regen. Med. 3:531–546; 2008.

29. Ng, F.; Boucher, S.; Koh, S.; Sastry, K. S.; Chase, L.; Lakshmipathy, U.; Choong, C.; Yang, Z.; Vemuri, M. C.; Rao, M. S.; Tanavde, V. PDGF, TGF-β, and FGF signaling is important for differentiation and growth of mesenchymal stem cells (MSCs): Transcriptional profiling can identify markers and signaling pathways important in differentia-tion of MSCs into adipogenic, chondrogenic, and osteo-genic lineages. Blood 112:295–307; 2008.

30. Oda, S.; Nishimatsu, S.; Murakami, K.; Ueno, N. Molecular cloning and functional analysis of a new activin beta sub-unit: A dorsal mesoderm-inducing activity in Xenopus. Biochem. Biophys. Res. Commun. 210:581–588; 1995.

31. Pangas, S. A.; Rademaker, A. W.; Fishman, D. A.; Woodruff, T. K. Localization of the activin signal transduction com-ponents in normal human ovarian follicles: Implications for autocrine and paracrine signaling in the ovary. J. Clin. Endocrinol. Metab. 87:2644–2657; 2002.

32. Pangas, S. A.; Woodruff, T. K. Activin signal transduction pathways. Trends Endocrinol. Metab. 11:309–314; 2000.

33. Picinich, S. C.; Mishra, P. J.; Mishra, P. J.; Glod, J.; Banerjee, D. The therapeutic potential of mesenchymal stem cells. Cell-tissue-based therapy. Expert Opin. Biol. Ther. 7:965–973; 2007.

34. Pittenger, M. F.; Mackay, A. M.; Beck, S. C.; Jaiswal, R. K.; Douglas, R.; Mosca, J. D.; Moorman, M. A.; Simonetti, D. W.; Craig, S.; Marshak, D. R. Multilineage potential of adult human mesenchymal stem cells. Science 284:143–147; 1999.

35. Raje, N.; Roodman, G. D. Advances in the biology and treatment of bone disease in multiple myeloma. Clin. Cancer Res. 17:1278–1286; 2011.

36. Santoro, M. M.; Gaudino, G. Cellular and molecular facets of keratinocyte reepithelization during wound healing. Exp. Cell Res. 304:274–286; 2005.

37. Sasaki, M.; Abe, R.; Fujita, Y.; Ando, S.; Inokuma, D.; Shimizu, H. Mesenchymal stem cells are recruited into wounded skin and contribute to wound repair by transdifferentiation into multiple skin cell type. J. Immunol. 180:2581–2587; 2008.

38. Sotiropoulou, P. A.; Papamichail, M. Immune properties of mesenchymal stem cells. Methods Mol. Biol. 407:225–243; 2007.

39. Tropel, P.; Noël, D.; Platet, N.; Legrand, P.; Benabid, A. L.; Berger, F. Isolation and characterization of mesenchymal stem cells from adult mouse bone marrow. Exp. Cell Res. 295:395–406; 2004.

40. Vallet, S.; Mukherjee, S.; Vaghela, N.; Hideshima, T.; Fulciniti, M.; Pozzi, S.; Santo, L.; Cirstea, D.; Patel, K.; Sohani, A. R.; Guimaraes, A.; Xie, W.; Chauhan, D.; Schoonmaker, J. A.; Attar, E.; Churchill, M.; Weller, E.; Munshi, N.; Seehra, J. S.; Weissleder, R.; Anderson, K. C.; Scadden, D. T.; Raje, N. Activin A promotes multiple myeloma-induced osteolysis and is a promising target for myeloma bone disease. Proc. Natl. Acad. Sci. USA 107:5124–5129; 2010.

41. Van Haastert, P. J.; Devreotes, P. N. Chemotaxis: Signaling the way forward. Nat. Rev. Mol. Cell Biol. 5:626–634; 2004.

42. Wankell, M.; Munz, B.; Hubner, G.; Hans, W.; Wolf, E.; Goppelt, A.; Werner, S. Impaired wound healing in transgenic mice overexpressing the activin antagonist follistatin in the epidermis. EMBO J. 20:5361–5372; 2001.

43. Werner, S.; Alzheimer, C. Roles of activin in tissue repair, fibrosis, and inflammatory disease. Cytokine Growth Factor Rev. 17:157–171; 2006.

44. Werner, S.; Grose, R. Regulation of wound healing by growth factors and cytokines. Physiol. Rev. 83:835–870; 2003.

45. Wu, Y.; Chen, L.; Scott, P. G.; Tredget, E. E. Mesenchymal stem cells enhance wound healing through differentiation and angiogenesis. Stem Cells 25:2648–2659; 2007.

46. Xia, Y.; Makris, C.; Su, B.; Li, E.; Yang, J.; Nemerow, G. R.; Karin, M. MEK kinase 1 is critically required for c-Jun N-terminal kinase activation by proinflammatory stimuli and growth factor-induced cell migration. Proc. Natl. Acad. Sci. USA 97:5243–5248; 2000.

47. Zhang, B.; Wang, F.; Deng, L.; Dun, A.; Dong, L.; Li, J.; Yang, H. Isolating and culturing rat marrow mesenchymal stem cells and studying their phenotypical and functional properties. Sichuan Da Xue Xue Bao Yi Xue Ban 34:738–741; 2003.

48. Zhang, F.; Tsai, S.; Kato, K.; Yamanouchi, D.; Wang, C.; Rafii, S.; Liu, B.; Kent, K. C. Transforming growth factor-beta promotes recruitment of bone marrow cells and bone marrow-derived mesenchymal stem cells through stimulation of MCP-1 production in vascular smooth muscle cells. J. Biol. Chem. 284:17564–17574; 2009.

49. Zhang, L.; Deng, M.; Kao, C. W.; Kao, W. W.; Xia, Y. MEK kinase 1 regulates c-Jun phosphorylation in the control of corneal morphogenesis. Mol. Vis. 9:584–593; 2003.

50. Zhang, L.; Deng, M.; Parthasarathy, R.; Wang, L.; Mongan, M.; Molkentin, J. D.; Zheng, Y.; Xia, Y. MEKK1 transduces activin signals in keratinocytes to induce actin stress fiber formation and migration. Mol. Cell. Biol. 25:60–65; 2005.

51. Zhang, L.; Wang, W.; Hayashi, Y.; Jester, J. V.; Birk, D. E.; Gao, M.; Liu, C. Y.; Kao, W. W.; Karin, M.; Xia, Y. A role for MEK kinase1 in TGF-beta/activin-induced epithelium movement and embryonic eyelid closure. EMBO J. 22:4443–4454; 2003.

52. Zhang, M.; Liu, N. Y.; Wang, X. E.; Chen, Y. H.; Li, Q. L.; Lu, K. R.; Sun, L.; Jia, Q.; Zhang, L.; Zhang, L. Activin B promotes epithelial wound healing in vivo through rhoA-JNK signaling pathway. PLoS One 6:e25143; 2011.